CrystEngComm

RSC Publishing

PAPER

View Article Online
View Journal | View Issue

Cite this: *CrystEngComm*, 2013, **15**, 5464

Can spherulitic growth rate accelerate before impingement for a semicrystalline polymer during the isothermal crystallization process?†

Shouyu Chen,[a] Yaqiong Zhang,[b] Huagao Fang,[b] Yunsheng Ding*[a] and Zhigang Wang*[b]

Received 8th March 2013,
Accepted 30th April 2013

DOI: 10.1039/c3ce40421h

www.rsc.org/crystengcomm

Isothermal crystallization processes in the temperature range from 110 to 140 °C were studied by using polarizing optical microscopy (POM) for poly(L-lactide) (PLLA) film samples with and without confinement conditions. The PLLA film samples were prepared by melt pressing between two cover glasses to provide the surface confinements and by removing the top cover glasses or by solution cast to keep the top surface free of confinements, respectively. Through carefully following the changes of spherulite radius with crystallization time, it is surprisingly found that there exists an acceleration of spherulitic growth rates at the late stage following the normal spherulitic growth rates at the early stage of isothermal crystallization for PLLA film samples with both surface confinement (by cover glasses) and planar confinement conditions (by aggregation of adjacent spherulites to form "lake-like" regions) at certain temperatures, while the spherulitic growth rates remain constant at each isothermal crystallization temperature for PLLA film samples without the confinement conditions. On the basis of data analyses on the spherulitic growth rates under various conditions from several different aspects, it is finally concluded that the decreases of glass transition temperature induced by crystallization under confinement conditions during isothermal crystallization of PLLA film samples cause the peculiar spherulitic growth rate acceleration at the late stage.

Introduction

Poly(L-lactide) (PLLA), belonging to the family of aliphatic polyesters, has attracted much attention because of its favorable biodegradability, transparency, nontoxicity to the human body and the environment, and versatile fabrication processes.[1,2] It is well known that the physical and mechanical properties of the semicrystalline polymers like PLLA are governed by the solid-state morphologies, which in turn are controlled by the crystallization process. In its amorphous form, the application of PLLA is limited by its low glass transition temperature (T_g), and for this reason only PLLA in crystalline forms can confer useful mechanical properties at temperatures higher than its T_g. However, the crystallization of PLLA is too slow to develop significant crystallinity, especially during normal processing conditions such as extrusion and injection molding, which has limited its development and wide practical applications. Poor processability, such as difficulty to demold, is also ascribed to its slow crystallization rate.[2] Therefore, how to improve the crystallization rate of PLLA has been an important topic, which has been paid attention to for a long while.

Crystallization can be considered to be an overall approach integrating the nucleation and growth mechanisms as well as the growth geometry. Crystallization of semicrystalline polymers consists of two stages: (i) nucleation stage, *i.e.*, the formation, within the liquid phase, of entities, called active nuclei, from which crystals appear, and (ii) growth stage, *i.e.*, the development stage of active nuclei into observable crystals. Accordingly, there are two methods, promoting nucleation rate and improving growth rate, respectively, to improve the crystallization rate. Consequently, it has been reported that addition of nucleating agent into PLLA to increase the nucleation density[3,4] or addition of plasticizers into PLLA[5] to increase crystal growth rate (to decrease the glass transition temperature) can effectively affect the crystallization kinetics of PLLA.

Crystallization kinetics of PLLA from melts has been extensively studied. Vasanthakumari and Pennings first studied the effects of molecular mass and crystallization temperature on the radial growth rate (G) of spherulites and

[a]*Institute of Polymer Materials & Chemical Engineering, School of Chemical Engineering, Provincial Key Laboratory of Advanced Functional Materials and Devices, Hefei University of Technology, Hefei, Anhui Province 230009, China. E-mail: zgwang2@ustc.edu.cn; dingys@hfut.edu.cn; Fax: +86 551-63607703; Tel: +86 551-63607703*

[b]*CAS Key Laboratory of Soft Matter Chemistry, Department of Polymer Science and Engineering, Hefei National Laboratory for Physical Sciences at the Microscale, University of Science and Technology of China, Hefei, Anhui Province 230026, China*

† Electronic supplementary information (ESI) available. See DOI: 10.1039/c3ce40421h

morphology of PLLA and carried out the analysis on the basis of the crystallization regime theory.[6] The temperature dependence of the spherulitic growth rate for PLLA has been particularly reported.[7–12] The first maximum of spherulitic growth rates for PLLA was observed at around 130 °C, while a second was observed at around 105 °C. The spherulitic growth rate showed clear discontinuity in the temperature range from 100 to 128 °C.[7–12] The appearance of discontinuity was reported to be dependent on molecular mass,[8,13] tacticity,[8] species for copolymerization,[8] and different crystalline forms.[10–12] This behavior had also been investigated by the regime transition from II to III,[7–9] because the slope ratio in the Hoffman–Lauritzen analysis is close to 2. However, other explanations were also provided recently by several research groups.[14,15] Although these researchers found discontinuity, the spherulitic growth rates were obtained incompletely from the relationships between spherulite radius and crystallization time during isothermal and/or nonisothermal crystallization processes. In this work the authors surprisingly find that there exist two different spherulitic growth rates under confinement conditions for PLLA film samples even at the same isothermal crystallization temperature. This singular discovery is specifically related to the crystallization behaviors of polymers under the confinement conditions. Two most recent significant findings as reported by our group have certain connections with this discovery. One is that Xu *et al.* found the existence of fluid flow in the undercooled melt during isothermal crystallization by following the motions of carbon black particles indwelt isotactic polypropylene (*i*PP) thin films.[16] Another one is that Wang *et al.* discovered the existence of translation and/or rotation of spherulites during the crystallization of *i*PP with reduced chain entanglements.[17] Thus, the origin of the peculiarity still remains as an open question and requires investigation for the complete understanding of the crystallization behaviors of PLLA.

Experimental

In this work the utilized poly(L-lactide) (PLLA, grade 4032D) was purchased from NatureWorks China/Hong Kong, Shanghai, China. The mass- and number-average molecular masses, M_w and M_n, were about 205 K and 115 K, respectively, and the polydispersity (M_w/M_n) is 1.78, measured by gel permeation chromatography (GPC, Waters 1515 with Waters 2414 RI detector and isocratic HPLC pump, U.S.A.).

Prior to any measurements PLLA pellets were dried under vacuum at 60 °C for 12 h. Then PLLA pellets were dissolved in chloroform with a mass concentration of 5 wt% at room temperature with stirring for 2 h, followed by precipitation in cyclohexane. The precipitated PLLA was dried under vacuum at 60 °C for 24 h and kept in a desiccator for further use.

The PLLA film samples for isothermal crystallization studies under confinements were prepared by pressing PLLA melts between two clean cover glasses into thin films with thicknesses of about 25–60 μm. Polarizing optical microscope (POM, Olympus BX51, Japan) equipped with a CCD camera (Tucsen TCC-3.3N, China) was used to observe the isothermal crystallization behaviors of PLLA film samples. Two home-made microscope hot stages provided the temperature control, with temperature uncertainty of ±0.1 °C. The PLLA film sample was first melted at 180 °C for 5 min on one hot stage to remove previous thermal histories and then was rapidly transferred to another hot stage kept at a certain crystallization temperature below the PLLA nominal melting point of 164 °C (determined at a heating rate of 10 °C min^{-1} by differential scanning calorimetry, DSC, Mettler Toledo DSC821e, Switzerland).

In order to compare with confinement conditions, PLLA film samples with a free top surface were prepared as follows. Drops of PLLA chloroform solution with concentration of 5 wt% were cast on cover glasses, which were kept in a tray with partial covering for controlled evaporation of chloroform for 12 h. Finally the PLLA film samples were dried under vacuum at 60 °C for 24 h. The isothermal crystallization studies on these PLLA film samples were also performed by following the same procedure for comparison purposes. In addition, for the PLLA film samples pressed between cover glasses, the top cover glasses were also taken off to obtain PLLA film samples without surface confinements, which were subjected to similar isothermal crystallization studies for comparison purposes.

The crystallization-induced glass transition temperature changes for PLLA film samples with and without confinements were examined by using differential scanning calorimetry (TA Q2000 DSC, TA Instruments, U.S.A.). PLLA film samples confined between cover glasses or cast on cover glasses with a free top surface were allowed to crystallize at different isothermal crystallization temperatures for certain times corresponding to the instants when the adjacent spherulites impinged upon each other to form liquid pockets, and then the PLLA film samples were quenched to room temperature by removing from the hot stage. The obtained PLLA film samples were then subjected to DSC measurements according to the following procedure: heating from 25 to 180 °C at a heating rate of 10 °C min^{-1}, kept at 180 °C for 5 min, rapidly cooling to 25 °C at a cooling rate of 50 °C min^{-1}, and then heating again from 25 to 180 °C at the rate of 10 °C min^{-1}. From the first and second heating scans the glass transition temperature changes can be estimated.

Results

For isothermal crystallization of PLLA in the studied temperature range from 110 to 140 °C, spherulites are the most common morphology. Fig. 1 presents the growths of spherulites during isothermal crystallization at 120 and 128 °C for PLLA film samples under confinements, that is to say, the PLLA film samples were sandwiched between the cover glasses. Fig. 2 indicates the selected spherulites and the selected spherulitic growth directions for measuring the changes of spherulite radius with crystallization time. By

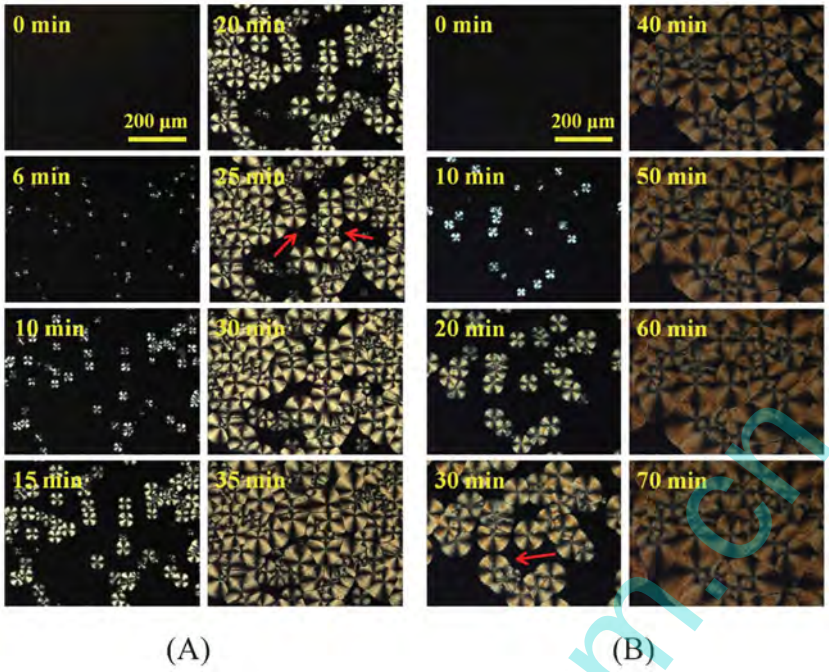

Fig. 1 Selected POM micrographs taken at different crystallization times during isothermal crystallization at (A) 120 °C and (B) 128 °C for PLLA film samples under confinements (sandwiched between cover glasses). The scale bars represent 200 μm and apply to all the micrographs.

plotting the changes of spherulite radius with time, the spherulitic growth rates can be obtained from the slopes of the fitted lines. Normally, a linearly fitted line can be obtained during the primary crystallization stage and a declined slope can be observed for the secondary crystallization stage.[18,19] However, it is quite interesting to see from Fig. 3 that for the isothermal crystallization of PLLA at 120 °C the changes of spherulite radius with time present a linear relationship at the early stage, while an acceleration of the growth rate of spherulites is clearly shown at the late stage. At the early stage the spherulites are small and they can grow larger separately at a low constant rate (defined as G_1). When spherulites start to aggregate through impinging upon each other at certain moments, several adjacent spherulites surround the undercooled melts to form liquid pockets (denoted as ''lake-like'' regions). From these moments on, the crystallization process is considered to enter into another stage where the slope between spherulite radius and time does not follow the foregoing linear relationship; instead, higher spherulitic growth rates appear (defined as G_2). This result is different from what people normally observe, that is to say, people normally observe the gradually slower and slower spherulitic growth rates at this late stage. From Fig. 3, we obtain four G_1 values of 2.1, 2.0, 2.0, 1.9 μm min^{-1} and four G_2 values of 2.5, 2.6, 2.2, 2.4 μm min^{-1}, corresponding to the four selected spherulites *a*, *b*, *c*, *d*, respectively, as indicated in Fig. 2(A). The average value of G_1 is 2.0 μm min^{-1} and that of G_2 is 2.4 μm min^{-1}. As for the separating points between the above two different growth rate stages, they are correlated to the aggregation of growing adjacent spherulites, which can be considered to provide a planar confinement for the further growth of spherulites, as will be discussed in detail in the later section.

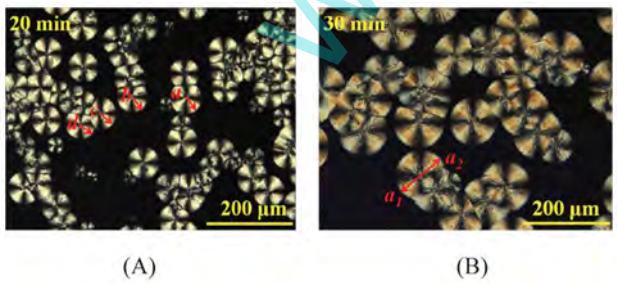

Fig. 2 Selected POM micrographs taken at (A) 120 °C and 20 min and (B) at 128 °C and 30 min during isothermal crystallization for PLLA film samples under confinements. The red arrows in (A) indicate the measured directions of the selected four spherulites and the red arrows in (B) indicate the two measured opposite directions of the selected one spherulite.

A similar phenomenon is also found for isothermal crystallization of PLLA film samples under confinements at other temperatures of 110, 113, 115, 118, 122 and 125 °C. Detailed information about the changes of radius of PLLA spherulites with crystallization time at the above temperatures can be found in the ESI† (Fig. S1–S21). When the temperature was set below 110 °C, the nucleation density of PLLA was so high that brought about difficulty in measuring the radii of spherulites precisely due to the high degree of undercooling.

When the crystallization temperature was set at 128 °C the nucleation density shown in Fig. 1(B) was relatively low

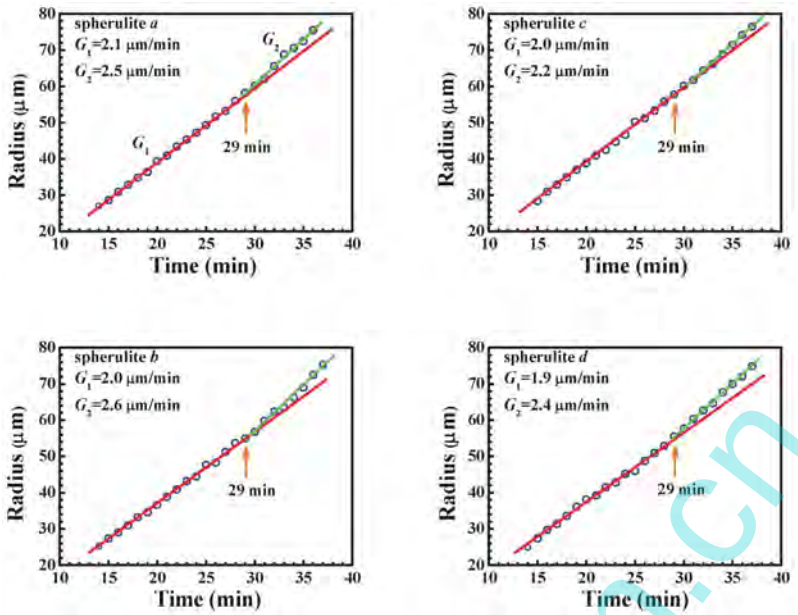

Fig. 3 Changes in radius of the selected four spherulites (*a*, *b*, *c* and *d*) as pointed out in Fig. 2(A) during isothermal crystallization at 120 °C for PLLA film sample under confinements.

because of relatively low degree of undercooling. We choose one peculiar spherulite as indicated in Fig. 2(B), which plays a similar role to a "dam" that controls the width of the "strait-like" flow channel in the crystallization process. Then we select two opposite radial directions of a_1 and a_2, which stand for two opposite spherulitic growing directions. With time, the right side of the spherulite along the a_2 direction enters into the "lake-like" region, while the left side of the spherulite along the a_1 direction is still immersed in the "sea-like" region. For these two opposite radial directions, it is interesting to see from Fig. 4 that the left side of the spherulite grows linearly over the time at a constant rate of 2.2 μm min^{-1} (G_1), while the right side of the spherulite grows at a lower rate of 2.0 μm min^{-1} (G_1) at the early stage before the flow channel is closed and grows at a higher growth rate of 2.3 μm min^{-1} (G_2) after the flow channel is closed. This result further confirms that the above two different growth rate stages are indeed related to the localization of the growing spherulites as aforementioned, due to the planar confinements, which affects further growth of spherulites.

The formation of liquid pockets results from the aggregation of adjacent spherulites, which is related to the nucleation density. Therefore, the shape and area of the liquid pockets are different for the PLLA film samples crystallized at different temperatures as shown in the POM micrographs (Fig. 1). When the isothermal crystallization temperatures were set at 130, 135 and 140 °C, the degree of undercooling for PLLA film samples were further reduced, leading to the much lower nucleation densities, which did not give rise to the possibility for the growing spherulites to form liquid pockets, and accordingly, no planar confinements could be introduced. With no such planar confinements, the spherulitic growth rates at the respective isothermal crystallization temperatures remain constant without any obvious deviations. The average spherulitic growth rates (G_1) at 130, 135 and 140 °C are 1.9, 1.6

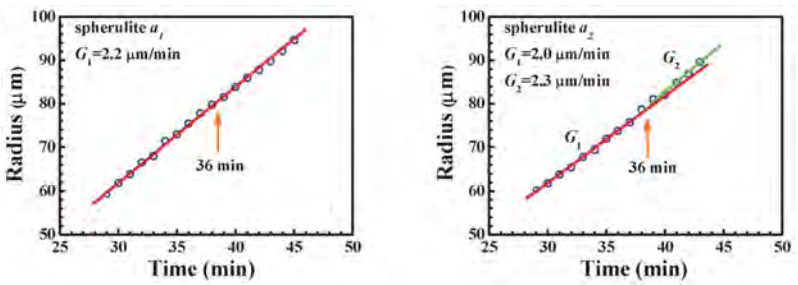

Fig. 4 Changes in radius of the selected spherulite during isothermal crystallization at 128 °C for PLLA film sample under confinements. Note that a_1 and a_2 stand for the two opposite spherulitic growth directions as pointed out in Fig. 2(B).

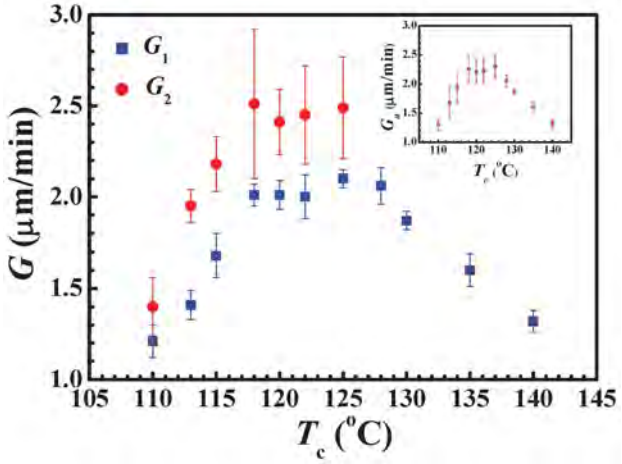

Fig. 5 Changes of spherulitic growth rates (G_1, G_2, and G_a in inset) as functions of isothermal crystallization temperature for PLLA film samples under confinements.

and 1.3 μm min^{-1}, respectively. Detailed information can be found in the ESI† (Fig. S25–S31).

Overall the spherulitic growth rates (G_1, G_2 and average rate G_a of G_1 and G_2) at different temperatures during isothermal crystallization for PLLA film samples under confinements are plotted in Fig. 5 (inset shows the average spherulitic growth rate, G_a of PLLA as a function of crystallization temperature). The spherulitic growth rates show the well-known bell-shaped temperature dependence, consistent with the classic crystallization theory, that is to say, G increases with increasing crystallization temperature, and after reaching a maximum, G decreases with further increasing crystallization temperature. A close examination indicates that the spherulitic growth rates of PLLA show discontinuity, no matter G_1, G_2 or G_a. The three growth rates show the same trend, namely, the spherulitic growth rate curves display the first maximum values at around 118 °C and the second maximum values at around 125 °C. Circumstantially, the spherulitic growth rates increase with increasing crystallization temperature and reach the first maximum values at around 118 °C, followed by a modest decrease. When crystallization temperature increases to exceed 120 °C, the spherulitic growth rates increase again to the second maximum values at around 125 °C, and then decrease with further increasing crystallization temperature. This result is analogous to that reported from other research groups,[7–12] however, their results only showed one singular growth rate curve.

For the purpose of comparison, the isothermal crystallization kinetics for PLLA film samples with a free top surface at different temperatures were studied. The PLLA film samples were prepared by solution cast on cover glasses, for which the surface confinements were absent. Fig. 6 shows the selected POM micrographs taken during isothermal crystallization at 120 °C for a PLLA film sample with a free top surface. The results for other crystallization temperatures can be found in the ESI.† Banded spherulites can be seen in Fig. 6 and 7. The

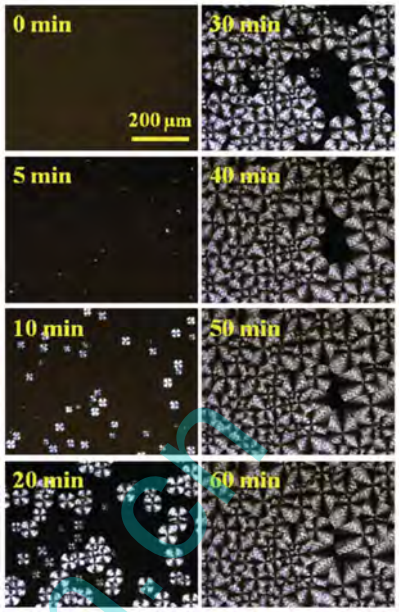

Fig. 6 Selected POM micrographs taken at different times during isothermal crystallization at 120 °C for PLLA film sample with free top surface. The scale bar represents 200 μm and applies to all the micrographs.

formation of banded spherulites for PLLA film samples with no surface confinements is complex and will be subjected to another detailed study in the future.[20–22] The nucleation density shown in Fig. 6 has no remarkable difference to that shown in Fig. 1(A). Some adjacent spherulites impinging upon each other to form the ''lake-like'' regions at the late stage can be seen as well. Fig. 8 shows the changes of spherulite radius over the entire crystallization time for the selected six spherulites shown in Fig. 7. It can be seen that the six spherulites all grow linearly with time with a nearly constant rate of 2.0 μm min^{-1}, which is about equal to G_1 at 120 °C as displayed in Fig. 3.

By the same way, we inspect the isothermal crystallization processes for PLLA film samples with no surface confinements (samples were prepared by solution cast) at 110, 115, 118, 120, 122, 125, 130, 135 and 140 °C, resulting in only one spherulitic

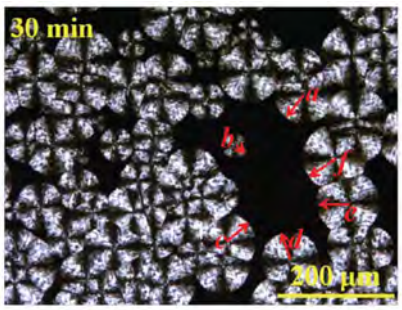

Fig. 7 Selected POM micrograph taken at 30 min during isothermal crystallization at 120 °C for PLLA film sample with free top surface. The six red arrows indicate the measured directions of the selected six spherulites, respectively.

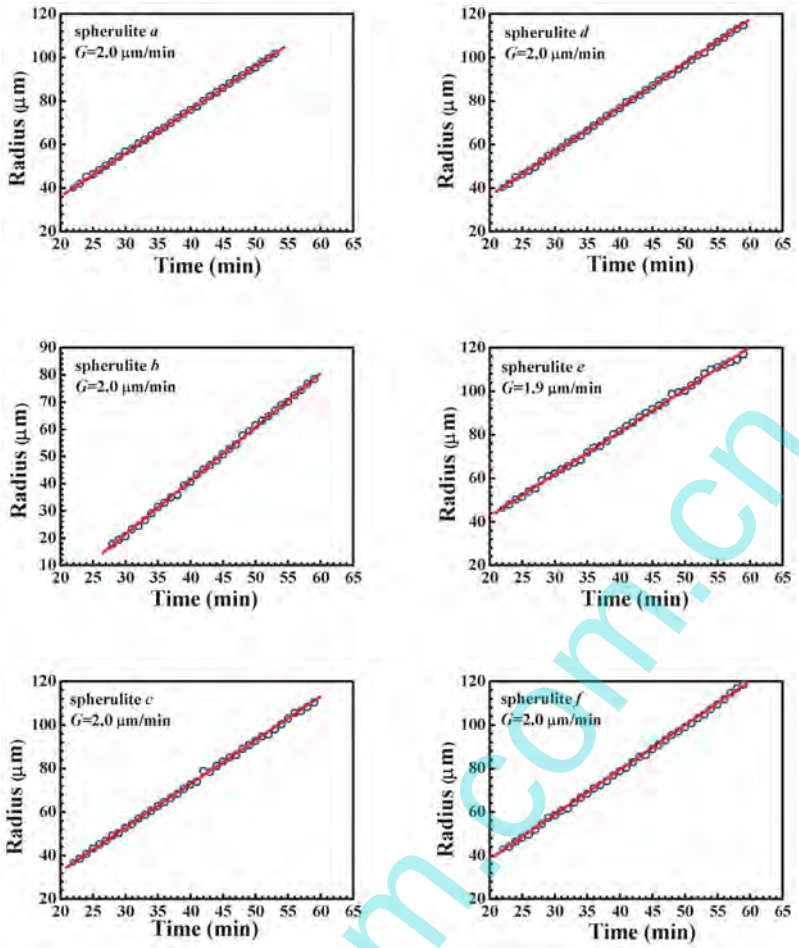

Fig. 8 Changes in radius of the selected six spherulites as indicated in Fig. 7 during isothermal crystallization at 120 °C for PLLA film sample with free top surface.

growth rate for each temperature, corresponding to 1.3, 1.5, 1.9, 2.0, 2.1, 2.1, 2.0, 1.9 and 1.7 μm min^{-1}, respectively. The detailed information can be found in the ESI† (Fig. S32–S58). The average spherulitic growth rates G_a at different temperatures during isothermal crystallization for PLLA film samples with no surface confinements are summarized in Fig. S59 and S60 of the ESI.† For the PLLA film samples pressed between cover glasses and then with the top cover glasses taken off, the isothermal crystallization data also show only one spherulitic growth rate for each isothermal crystallization temperature, and the detailed information can be found in the ESI† (Fig. S61–S69). The average spherulitic growth rates G_a at different temperatures during isothermal crystallization for this type of PLLA film samples with no surface confinements are summarized in Fig. S70 and S71 of the ESI.†

Discussion

For the surface confinement conditions, two spherulitic growth rates at certain temperatures for PLLA film samples are clearly observed, which naturally leads to the questions of what causes the phenomenon during isothermal crystallization and what are the requirements to bring forth the unique phenomenon.

First of all, we consider the possible influence of molecular masses of the PLLA samples. Several papers had reported that PLLA with a lower molecular mass had a higher growth rate than that with a higher molecular mass.[7,8,13] Our PLLA sample has the polydispersity of 1.78, which is relatively wide. Perhaps the PLLA chains with high molecular masses crystallize first, and then the PLLA chains with low molecular masses start to crystallize with a higher spherulitic growth rate? If this is the case, the PLLA film samples with the free top surface showing only one spherulitic growth rate at each crystallization temperature cannot be explained. In addition, whether or not degradation of PLLA takes place during crystallization needs to be examined. We did the GPC measurement on the PLLA sample having crystallized at 140 °C for 2 h and found the molecular masses and polydispersity of the PLLA sample did not show any obvious changes. Furthermore, only one spherulitic growth rate was observed for PLLA film sample under the confinement condition at 140 °C. We thus conclude that molecular masses and polydispersity of PLLA should not cause the observed phenomenon.

As above mentioned, several papers had reported the discontinuity of spherulitic growth rate for PLLA and had explained it by the changes of crystal form.[10–12] Studies by Kawai and co-workers[12] have shown that PLLA crystallizes as α-form crystals when the crystallization temperature T_c is higher than 120 °C and crystallizes as the α′-form crystals when the crystallization temperature T_c is lower than 90 °C. Studies by Pan and co-workers[11] have shown that at $T_c \geqslant 110$ °C and $T_c < 110$ °C, the α-form and α′-form crystals are mainly produced, respectively. Studies by Yasuniwa and co-workers[10] have shown that crystal structures for PLLA samples isothermally crystallized at temperatures higher and lower than 113 °C are orthorhombic (α-form) and trigonal (β-form), respectively. From the results of these papers and the others, it can be thought that crystal forms might be different at different T_c, but they should remain exclusive at certain temperatures. Therefore, there is no crystal form transformation that leads to the spherulitic growth rate acceleration at the late crystallization stage under the surface confinement conditions at certain isothermal crystallization temperature.

Then we consider the effect of crystallization regime transition according to the Hoffman–Lauritzen analysis.[7–9] On the basis of the nucleation theory established by Lauritzen and Hoffman, the crystal growth rate G at the crystallization temperature T_c can be expressed by eqn (1) as follows:

$$G(T) = G_0 \exp\left(-\frac{U^*}{R(T_c - T_\infty)}\right) \exp\left(-\frac{K_g}{T_c \Delta T f}\right) \quad (1)$$

where G_0 is the pre-exponential factor, U^* is the activation energy for transport of chain segments to the site of crystallization, R is the gas constant, T_c is the crystallization temperature, T_∞ is the hypothetical temperature where all motions associated with viscous flow cease, ΔT is the degree of undercooling given by $T_m^o - T_c$ where T_m^o is the equilibrium melting point, f is a factor, which accounts for the variation in the enthalpy of fusion as the temperature is decreased below T_m^o, given by $f = 2T_c/(T_m^o + T_c)$, and K_g is a nucleation constant. The T_m^o value of 210.5 °C is obtained for the PLLA sample in this study by applying the Hoffman–Weeks method (see Fig. S72 of the ESI†). This value of T_m^o approximates those reported by Xiao *et al.*,[23] Park *et al.*[24] and Castillo *et al.*[25] The empirical universal values of U^* = 1500 cal mol^{-1} and $T_\infty = T_g - 30$ K where T_g is 334.5 K, which is the average value of T_g obtained from the second heating scan in DSC measurements (shown later in Fig. 11), are applied for the regime analysis of the PLLA crystallization.

The regime transition can be demonstrated from the kinetic treatment according to eqn (1) by plotting ln $G + U^*/R(T_c - T_\infty)$ as a function of $1/(T_c \Delta T f)$. The existence of different regimes can be identified by the change of the slope of the fitted lines, which are the values of the nucleation constant K_g at different regimes. Fig. 9 shows the plot of ln $G + U^*/[R(T_c - T_\infty)]$ as a function of $10^5/(T_c \Delta T f)$. It can be seen that G_1, G_2 and G_a follow linear relationships with the slopes of −3.34, −3.74 and −3.55, respectively. The three K_g values of 3.34 × 10^5, 3.74 × 10^5 and 3.55 × 10^5 K^2 are close to the values of K_g(II) as

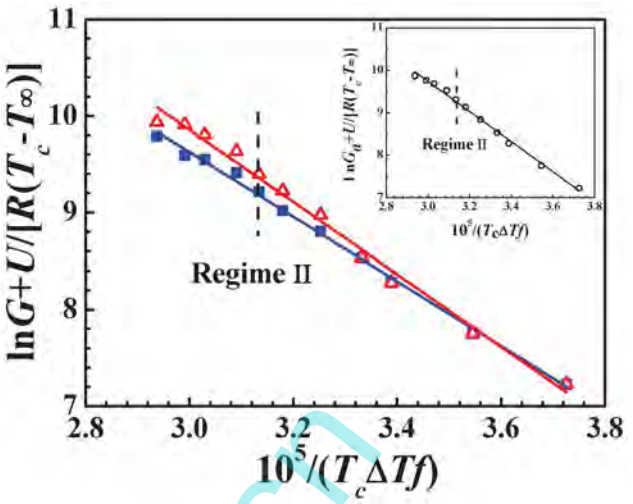

Fig. 9 Kinetic analysis of spherulitic growth rates for PLLA film samples under confinements. Blue square and red triangle data points are obtained from G_1 and G_2, respectively. Inset shows the plot of ln $G_a + U^*/[R(T_c - T_\infty)]$ as a function of $10^5/(T_c \Delta T f)$ for PLLA film samples.

reported in the literature.[6–8] These results indicate that PLLA utilized in this study crystallizes solely according to the regime II kinetics for all the T_c values (110–140 °C) and no apparent regime I to II and regime II to III transitions can be observed. The regime transitions are affected by molecular mass, tacticity and comonomer contents of PLLA as reported by Tsuji *et al.*[8] The D-isomer lactide in the PLLA sample (PLLA-4032D) in this study is about 1.3%,[4,26] so the regime II to III transition temperature ($T_{c(II–III)}$) should be slightly higher than 110 °C, which is the lowest temperature in our studied temperature range. Some studies reported that for the PLLA-4032D samples with the D-isomer lactide contents of 4.4%[27] or 10%[28] the $T_{c(II–III)}$ values are even lower than 110 °C. Thus, the absence of the regime II to III transition in our study compared with the reported $T_{c(II–III)}$ value of 120 °C[7,8,12] (marked by the dashed line in Fig. 9) comes from the different used PLLA samples. The above result indicates that the theory of crystallization regime transitions cannot be used to explain the observed spherulitic growth rate acceleration phenomenon.

The critical condition piercing through the entire observation is that several adjacent spherulites aggregate through impinging upon each other to form the liquid pockets for the PLLA film samples covered with top cover glasses. It is considered that the surface spherulitic morphology under the cover glass might provide some clues. Thus, we conducted an AFM measurement (AFM, CSPM5000, Benyuan, Beijing, China) on the PLLA film sample that was sandwiched between two cover glasses and then the top cover glass was removed after the completion of crystallization at 110 °C for 30 min. The AFM height image (Fig. S73 of the ESI†) indicates that the height at the crystal growth front of the spherulites decreases gradually from the center in pace with the spherulitic growth. Mackay *et al.*[29] reported the melt density of 1.09 g cm^{-3} at 200

°C for PLLA, Dorgan *et al.*[30] reported the density of 1.16 g cm^{-3} at 180 °C for PLLA, and the PLLA manufacturer provided us the density of 1.24 g cm^{-3} for PLLA pellets in this study. The slight density difference between melts and crystals and the gradual height decrease of spherulitic front for PLLA film samples demonstrate that sufficient undercooled melt can be supplied to the growth front of spherulites. Because we did not observe any cavitations or apparent defects in the spherulites at the late stage of crystallization, the cavitation or defect mechanisms cannot be used to explain the spherulitic growth rate acceleration at the late crystallization stage under the surface confinement conditions.

Spherulite is the basic higher order structure for polymer crystallization from melts or concentrated solutions.[31] With the development of crystallization, there exists fluid flow or a build-up of local negative hydrostatic pressure. Several papers have reported the experimental results.[16,32–34] Among these, Xu *et al.*[16] had attributed the reason to the process of fluid flow during isothermal crystallization for *i*PP under confinements. In their study, they found that there existed a large local negative hydrostatic pressure due to crystallization, the relaxation of these inhomogeneous stresses could induce fluid flow with confinement conditions, and fluid flow was arrested at the later times when the spherulites impinged upon each other. When removing the confinement conditions, the local stresses could simply relax at the free polymer surface, and polymer film thinning occurred instead of building-up of local negative pressure within the film as crystallization progressed. We also used the optical microscope to observe the PLLA fluid flow during isothermal crystallization at different temperatures (from 120 to 135 °C) for PLLA film samples under surface confinement conditions by following the motions of some graphene oxide particles (black color) indwelt PLLA thin films, and the results demonstrate an obvious fluid flow (at the temperatures from 120 to 128 °C) and a slight fluid flow (at the temperatures of 130 and 135 °C) for PLLA isothermal crystallization under surface confinement conditions; in contrast, the absence of fluid flow is confirmed at all the studied temperatures (from 120 to 135 °C) when the surface confinements were removed.

In our study, PLLA spherulites continue to grow with a higher rate after spherulites aggregate (analogue to a type of percolation) to form the liquid pockets under surface confinement conditions; however, the spherulites only grow linearly with one constant rate when removing the surface confinement conditions. We must notice the effect of nucleus density for the above two cases. The aggregation of spherulites to form liquid pockets needs a sufficient nucleus density. For the PLLA film samples with and with no top cover glasses, respectively, the difference of nucleus density at each isothermal crystallization temperature is noticeable, with relatively higher nucleus densities found for the former than the latter possibly due to certain nucleation ability of the top cover glass for PLLA crystallization (see Table S1 and Fig. S74–S75 of the ESI†). However, the cover glass nucleation ability is considered less effective than the homogeneous nucleation ability of PLLA because the cover glass shows hydrophilic property, whereas the PLLA film is hydrophobic; in addition, the nucleation density difference is negligible regarding the much lower nucleus number than the observed nucleus density required for aggregation of spherulites to form liquid pockets during isothermal crystallization, especially at the relatively low temperatures, for which the spherulitic growth rate acceleration is more obvious (see Fig. S1–S53 of the ESI†). From the above analyses, we confirm that the crucial factor causing the accelerated spherulitic growth rate is the surface confinement conditions and the aggregation of spherulites to form liquid pockets. Before impinging of spherulites, the undercooled melt can flow to eliminate the local stresses at the melt/crystal interface. After the aggregation of spherulites, the local stresses cannot relax. The local stresses and space confinements due to aggregation of spherulites during crystallization have a certain relationship with the polymer chain segment mobility, which can be characterized by the changes of glass transition temperature, which will be discussed in the following sections.

Crystallization of polymer is the process of chain segment rearrangements, thus, the spherulitic growth rate is correlated with the polymer chain segment mobility, which is usually characterized by the glass transition temperature (T_g). Therefore, the question comes whether the confinement conditions during PLLA crystallization increase the PLLA chain segment mobility or not when the aggregation of spherulites occurs, which then accelerates the spherulitic growth rate? If this does happen, the characteristic parameter, T_g, which indicates the PLLA chain segment mobility, might be decreased to some degree. Surprisingly, some clues for this bold assumption are found in two reported cases from the literature. The first one is that Mäder *et al.*[34] studied the two-phase melt blends consisting of polypropylene (PP) and elastomers such as styrene-*b*-(ethylene-*co*-butylene)-*b*-styrene triblock copolymer (SEBS), and poly(ethylene-*co*-1-octene) (PEO), and they found that there existed depression of T_g for PP/elastomer blends with respect to T_g of the corresponding neat elastomer because of thermally induced internal stress resulting from differential volume contraction of the two phases during cooling from melts. The second one is more interesting because the studied polymer materials are PLLA samples.[35] For neat PLLA, Fitz *et al.*[35] reported significant reductions in T_g for PLLA crystallized under partially constrained conditions, in which PLLA films were prevented from shrinking and the constrained crystallization process resulted in increase of the free volume in the amorphous phase. Referring to the above two reports, the DSC measurements were performed on the PLLA samples, which had crystallized at certain times corresponding to the instants when the PLLA spherulites began to impinge upon each other to form liquid pockets. Fig. 10(a) shows the DSC heat flow curves during the first heating scan for PLLA samples crystallized between cover glasses for certain times when the spherulites began to impinge upon each other at different isothermal crystallization temperatures. Fig. 10(b) shows the DSC heat flow

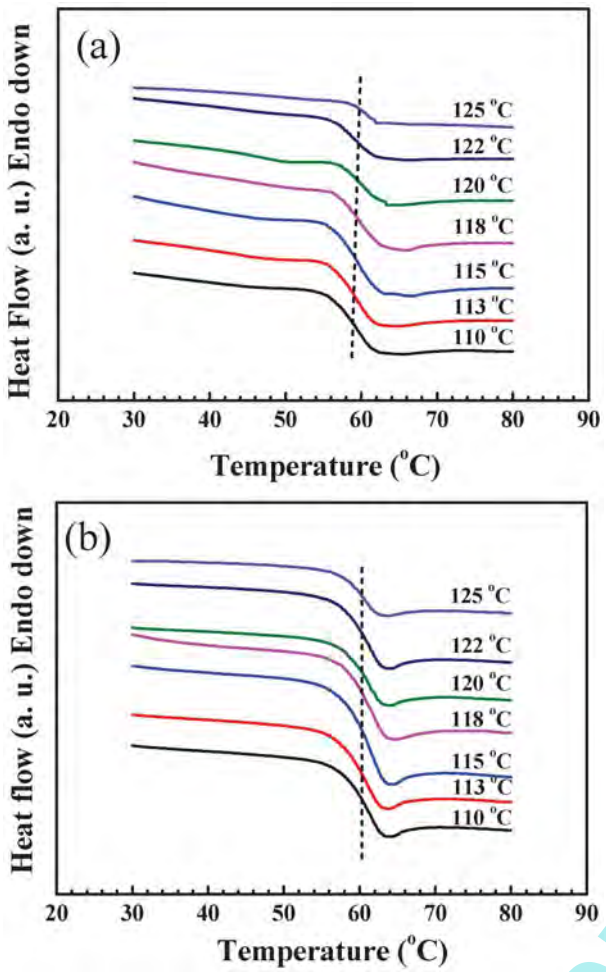

Fig. 10 (a) DSC heat flow curves during the first heating scan with a heating rate of 10 °C min^{-1} for PLLA samples, which had crystallized between cover glasses for certain times when the spherulites began to impinge upon each other at different temperatures. (b) DSC heat flow curves during the second scan with a heating rate of 10 °C min^{-1} for PLLA samples from (a), which were remained at 180 °C for 5 min and then quenched to 30 °C at a cooling rate of 50 °C min^{-1}. The applied crystallization temperatures are marked above the curves.

curves during the second heating scan for PLLA samples from Fig. 10(a), which were maintained at 180 °C for 5 min and then quenched to 30 °C at a cooling rate of 50 °C min^{-1}. The short dashed lines mark the glass transition temperatures on the heat flow curves, which indicate the relatively lower T_g values for the first heating scan than the second heating scan. The changes of T_g for the first heating scan (defined as T_{gc}) and for the second heating scan (defined as T_{gf}) with the isothermal crystallization temperature for PLLA samples are shown in Fig. 11. It can be clearly seen that T_{gc} values are lower than T_{gf} values. When the PLLA film sample sandwiched between two cover glasses crystallized at T_c below 128 °C, the undercooled melt fluid cannot flow any more when spherulites impinge upon each other to form liquid pocket regions at the late stage of crystallization, and then the crystallization-induced internal stresses cannot relax because of space confinements. Therefore, the undercooled amorphous melt phase cannot

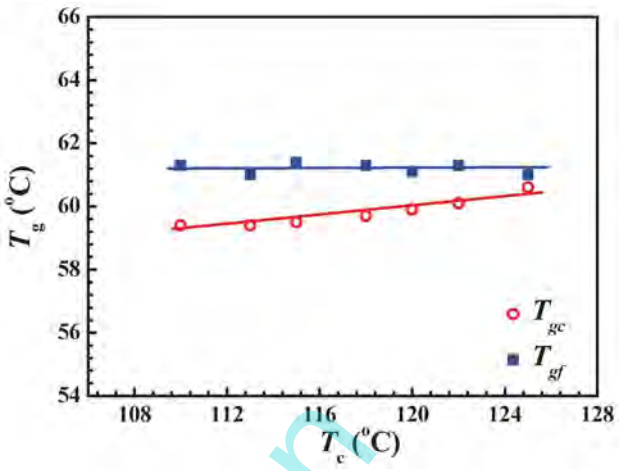

Fig. 11 Changes of glass transition temperature, T_g with isothermal crystallization temperature, T_c for PLLA samples during the first heating scan (T_{gc}) and the second heating scan (T_{gf}).

shrink freely, which leads to increasing free volume in the amorphous phase. Thus, the PLLA chain segment mobility can be enhanced, reflected by the decreasing T_g values as measured from the first heating scan by DSC. After the PLLA samples are melted in the DSC pans, the previous internal stresses induced by confinements between cover glasses will be eliminated, and then the second heating scan by DSC measurements can provide the normal T_g values for these samples. The T_{gc} values for all PLLA samples that are confined are lower than T_{gf} values for PLLA samples that are released from the confinements. In addition, T_{gf} shows much less change than T_{gc} with increasing crystallization temperature, T_c as shown in Fig. 11, because the crystallization-induced confinement degree is certainly related to the crystallization temperature. Fig. 11 also indicates that the difference between T_{gf} and T_{gc} becomes smaller with increasing crystallization temperature. The PLLA film sample crystallized between cover glasses for certain time at 135 °C was further measured by DSC and the result shows similar T_{gf} and T_{gc} values (see Fig. S76 in the ESI†). For comparison purposes, the PLLA samples with free top surface obtained from solution cast were examined by DSC measurements in the same way and the results show that the glass transition temperatures do not show obvious decreases because of the absence of confinements (see Fig. S77 and Table S2 in the ESI†).

We can now return to the kinetic analysis of the spherulitic growth rates for PLLA film samples under confinements as shown in Fig. 9. The spherulitic growth rate, G, at the crystallization temperature, T_c, follows the nucleation theory of the Hoffman–Lauritzen model. That is to say, the red triangle data points in Fig. 9 should be close to the blue square data points or the blue curve, and the slopes of the two lines should have little difference for the same PLLA material. Our above DSC experimental results have demonstrated that the glass transition temperature decreases at the late stage of crystallization for PLLA film samples having the surface

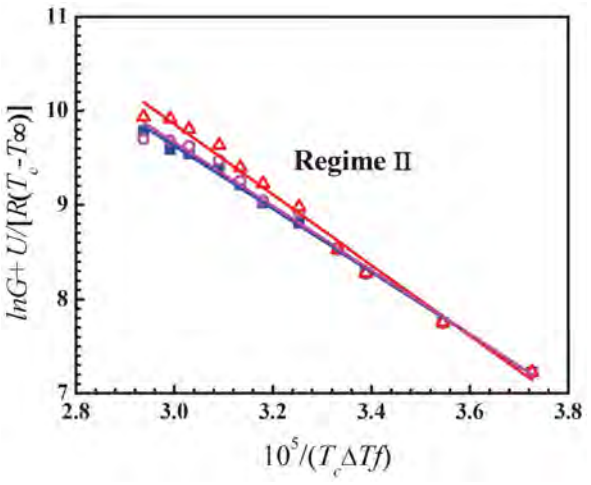

Fig. 12 Kinetic analysis on the spherulitic growth rates for PLLA film samples under confinements through modification of the glass transition temperatures. Blue square and red triangle data points are obtained from G_1 and G_2, respectively. Magenta open circle data points are obtained from G_2 by adopting T_{gc} obtained from the first heating scan as shown in Fig. 10 and 11.

confinement and planar confinement. Thus, on the other hand, we can prove that the spherulitic growth rate acceleration is related to the decrease of T_g by changing the values of glass transition temperature, T_g, in accordance with eqn (1) to shift down the red triangle data points based on G_2. Fig. 12 shows the result. It can be seen that the magenta open circle data points (the shifted red triangle data points) are now close to the blue square data points and the slope for the magenta open circle data points is -3.39, which is much closer to -3.34 for the slope of the blue square data points, when compared with -3.74 for the slope of the red triangle data points. This analysis provides a strong evidence to support the phenomenon of spherulitic growth rate acceleration at the late stage of crystallization.

Fig. 13 schematically summarizes the typical growth of spherulites and decrease of glass transition temperature induced by crystallization under confinements. At the initial stage, nucleation starts randomly in the polymer melt and the spherulites grow radially in all directions with about the same rates, as shown in Fig. 13(a). For the sake of simplification, it is assumed that the spherulites start to grow at the same time. In reality the sizes of spherulites are different because the nuclei start at different times. The spherulites in thin films (usually for optical microscope observations) are not spherical entities, which grow more or less in the two-dimensional film plane. At the moment, the degree of crystallinity is relatively low and the melt is the continuous phase, thus the polymer chain segments can freely move. The glass transition temperature can be designated as T_{gf}. With crystallization proceeding, small spherulites grow larger and larger, and eventually several adjacent spherulites impinge upon each other to form liquid pockets as shown in Fig. 13(b). The state of the polymer chain segments in the amorphous phase of liquid pockets may be different from the foregoing state, because from this moment the stresses in the undercooled melt, confined by both spherulites and the cover glasses, cannot relax. When crystallization continues further, the undercooled melt will be stretched because of the nearly fixed thickness of the confined film and the fixed sample volume, in which there is an increasing crystalline volume fraction with a higher density than the amorphous fraction. In other words, the space for the polymer chain segments to move can be increased. Therefore, the net free volume in the amorphous phase of the liquid pockets will increase. Accordingly, the glass transition temperature, designated as T_{gc}, becomes lower than T_{gf}. The decrease of glass transition temperature can eventually cause the acceleration of the spherulitic growth rate from this moment on. We note that there was only less than 2 μm thickness thinning after crystallization and compared with the thicknesses of the film samples (25–60 μm) before crystallization, the decrease was considered to be negligible. Therefore, the thicknesses of the confined PLLA films were considered to be nearly fixed during crystallization.

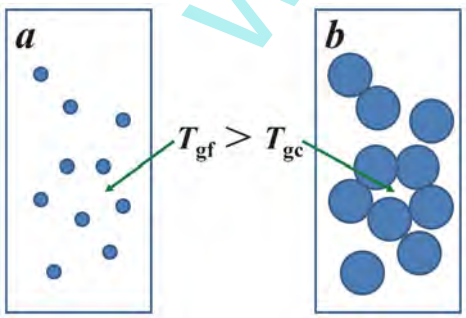

Fig. 13 Schematic of the nucleation and growth of spherulites and the related decrease of glass transition temperature induced by crystallization due to the confinements in the liquid pocket region.

During exploring the reasons for the spherulitic growth rate acceleration under confinements during PLLA isothermal crystallization, we find that the key factor is the confinement conditions, which decrease the glass transition temperature in the confined amorphous regions. In practical industrial productions, such as extrusion, injection molding, calendaring, melt fiber spinning, film blowing *etc.*, there exist crystallization-induced confinements in the polymer materials in the production facilities before accomplishment of production. Therefore, our results might have certain guidance for producing polymer products with admired physical properties through the intended appropriate controlling of the crystallization-induced confinements, especially for the products involving the semicrystalline polymer thin films.

Conclusions

Isothermal crystallization for PLLA film samples with and without surface confinements in the temperature range from 110 to 140 °C was carefully studied by using polarizing optical

microscope. The results show that for the PLLA film samples prepared by pressing PLLA melts between two cover glasses, there exists an acceleration of the spherulitic growth rates at the late stage following the normal spherulitic growth rates at the early stage of isothermal crystallization in the temperature range from 110 to 125 °C, and there exists only one spherulitic growth rate for each crystallization temperature above 128 °C. However, if the PLLA film samples with no surface confinements were prepared by solution cast or by pressing PLLA melts between two cover glasses and then removing the top cover glass, there exists also only one spherulitic growth rate for each isothermal crystallization temperature in the whole studied range. We find that the appearance of acceleration of the spherulitic growth rate is due to the confinement conditions, which are formed between the two cover glasses (surface confinement) and aggregation of adjacent spherulites to produce the ''lake-like'' regions (planar confinement). Although molecular mass and crystal form transformation can influence the spherulitic growth rate, they should not function at a certain crystallization temperature. Further analyses of the spherulitic growth rates on the basis of the Hoffman–Lauritzen model and of the surface morphology of spherulites by AFM observation demonstrate that the stresses induced by crystallization play the key role in the spherulitic growth rate acceleration at the late stage of crystallization. More specifically, for the PLLA film samples with surface confinement, the undercooled melts can flow to release the stresses at the early stage of crystallization. Once adjacent spherulites aggregate through impinging upon each other to form the liquid pockets (the ''lake-like'' regions), the entrapped undercooled melts cannot flow any more, and the stresses cannot be eliminated. Then the undercooled amorphous melts cannot shrink freely and the net free volume in the amorphous phase increases. Hence, the glass transition temperature, T_g, in the ''lake-like'' regions decreases, which causes the spherulitic growth rate acceleration in the late stage of crystallization. For the PLLA film samples with no confinement conditions, the spherulitic growth rates remain constant during isothermal crystallization because of releasing of the stresses and the constant glass transition temperature. The peculiar results reported here might guide PLLA production in order to obtain more appropriate properties by intended appropriate controlling of the crystallization-induced inner stresses.

Acknowledgements

ZGW acknowledges the financial support from the National Science Foundation of China (No. 21174139) and National Basic Research Program of China (No. 2012CB025901) and YSD acknowledges the financial support by the National Science Foundation of China (No. 50973025).

References

1 D. Garlotta, *J. Polym. Environ.*, 2001, **9**, 63–84.
2 L. T. Lim, R. Auras and M. Rubino, *Prog. Polym. Sci.*, 2008, **33**, 820–852.
3 X. Hu, H. N. An, Z. M. Li, Y. Geng, L. B. Li and C. L. Yang, *Macromolecules*, 2009, **42**, 3215–3218.
4 Z. H. Xu, Y. H. Niu, Z. G. Wang, H. Li, L. Yang, J. Qiu and H. Wang, *ACS Appl. Mater. Interfaces*, 2011, **3**, 3744–3753.
5 H. Li and M. A. Huneault, *Polymer*, 2007, **48**, 6855–6866.
6 R. Vasanthakumari and A. J. Pennings, *Polymer*, 1983, **24**, 175–178.
7 H. Abe, Y. Kikkawa, Y. Inoue and Y. Doi, *Biomacromolecules*, 2001, **2**, 1007–1014.
8 H. Tsuji, Y. Tezuka, S. K. Saha, M. Suzuki and S. Itsuno, *Polymer*, 2005, **46**, 4917–4927.
9 D. L. M. Laura, *Eur. Polym. J.*, 2005, **41**, 569–575.
10 M. Yasuniwa, S. Tsubakihara, K. Iura, Y. Ono, Y. Dan and K. Takahashi, *Polymer*, 2006, **47**, 7554–7563.
11 P. Pan, B. Zhu, W. Kai, T. Dong and Y. Inoue, *J. Appl. Polym. Sci.*, 2008, **107**, 54–62.
12 T. Kawai, N. Rahman, G. Matsuba, K. Nishida, T. Kanaya, M. Nakano, H. Okamoto, J. Kawada, A. Usuki, N. Honma, K. Nakajima and M. Matsuda, *Macromolecules*, 2007, **40**, 9463–9469.
13 T. Miyata and T. Masuko, *Polymer*, 1998, **39**, 5515–5521.
14 D. L. M. Laura, *Polymer*, 2001, **42**, 9441–9446.
15 M. L. Di Lorenzo, *Macromol. Symp.*, 2006, **234**, 176–183.
16 D. H. Xu, Z. G. Wang and J. F. Douglas, *Macromolecules*, 2007, **40**, 1799–1802.
17 X. Wang, Z. Wang, K. Luo and Y. Huang, *Macromolecules*, 2011, **44**, 2844–2851.
18 L. Chang and E. M. Woo, *Polymer*, 2011, **52**, 68–76.
19 K. M. Kit, *Polymer*, 1998, **39**, 4969–4971.
20 J. Xu, B. H. Guo, J. J. Zhou, L. Li, J. Wu and M. Kowalczuk, *Polymer*, 2005, **46**, 9176–9185.
21 H. Kajioka, A. Hoshino, H. Miyaji, Y. Miyamoto, A. Toda and M. Hikosaka, *Polymer*, 2005, **46**, 8717–8722.
22 T. Wang, H. Wang, H. Li, Z. Gan and S. Yan, *Phys. Chem. Chem. Phys.*, 2009, **11**, 1619–1627.
23 H. Xiao, F. Liu, T. Jiang and J. T. Yeh, *J. Appl. Polym. Sci.*, 2010, **117**, 2980–2992.
24 J. W. Park and S. S. Im, *J. Appl. Polym. Sci.*, 2002, **86**, 647–655.
25 R. V. N. Castillo, A. J. Müller, M. C. Lin, H. L. Chen, U. S. Jeng and M. A. Hillmyer, *Macromolecules*, 2008, **41**, 6154–6164.
26 Z. Xu, Y. Zhang, Z. Wang, N. Sun and H. Li, *ACS Appl. Mater. Interfaces*, 2011, **3**, 4858–4864.
27 E. Manfredi, F. Meyer, P. Verge, J.-M. Raquez, J. M. Thomassin, M. Alexandre, B. Dervaux, F. DuPrez, P. Van Der Voort, C. Jerome and P. Dubois, *J. Mater. Chem.*, 2011, **21**, 16190–16196.
28 A. L. Goffin, E. Duquesne, J. M. Raquez, H. E. Miltner, X. Ke, M. Alexandre, G. Van Tendeloo, B. Van Mele and P. Dubois, *J. Mater. Chem.*, 2010, **20**, 9415–9422.
29 J. J. Cooper-White and M. E. Mackay, *J. Polym. Sci., Part B: Polym. Phys.*, 1999, **37**, 1803–1814.
30 J. R. Dorgan, J. S. Williams and D. N. Lewis, *J. Rheol.*, 1999, **43**, 1141–1155.

31 L. Gránásy, T. Pusztai, G. Tegze, J. A. Warren and J. F. Douglas, *Phys. Rev. E: Stat. Phys., Plasmas, Fluids, Relat. Interdiscip. Top.*, 2005, **72**, 011605.
32 A. Toda, K. Taguchi and H. Kajioka, *Macromolecules*, 2008, **41**, 7505–7512.
33 R. Thomann, C. Wang, J. Kressler and R. Mülhaupt, *Macromol. Chem. Phys.*, 1996, **197**, 1085–1091.
34 D. Mäder, M. Bruch, R.-D. Maier, F. Stricker and R. Mülhaupt, *Macromolecules*, 1999, **32**, 1252–1259.
35 B. D. Fitz, D. D. Jamiolkowski and S. Andjelić, *Macromolecules*, 2002, **35**, 5869–5872.